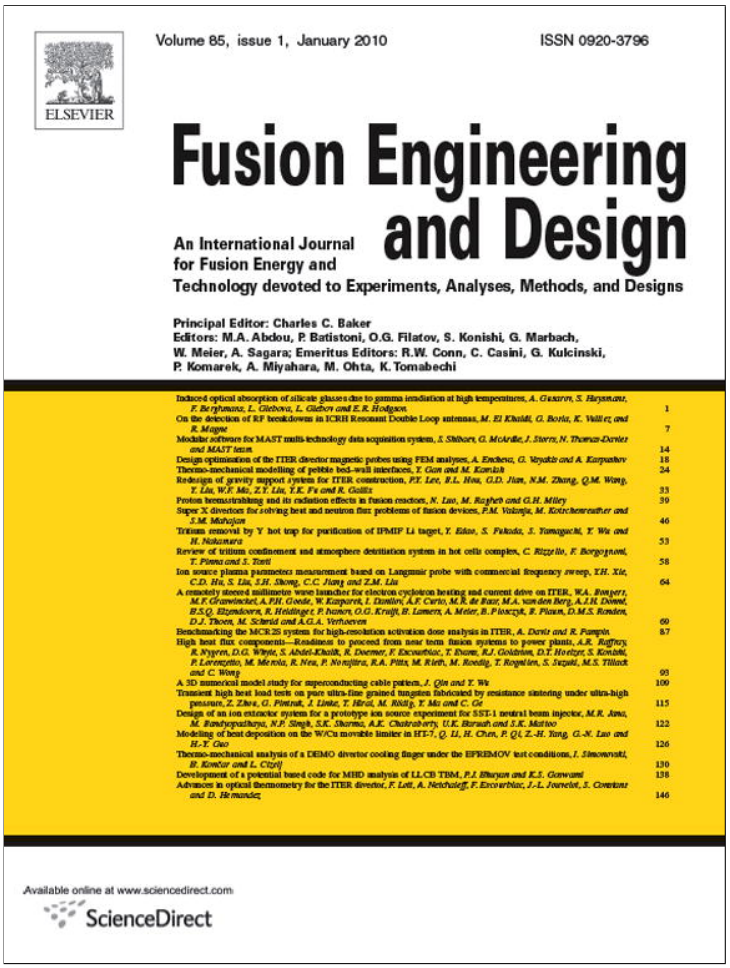

Fusion Engineering and Design 85 (2010) 24–32

Contents lists available at ScienceDirect

Fusion Engineering and Design

journal homepage: www.elsevier.com/locate/fusengdes

Thermo-mechanical modelling of pebble bed–wall interfaces

Yixiang Gan*, Marc Kamlah

IMF II, Forschungszentrum Karlsruhe, 76344, Eggenstein-Leopoldshafen, Germany

ARTICLE INFO

Article history:
Received 7 November 2008
Received in revised form 6 May 2009
Accepted 26 May 2009
Available online 24 June 2009

Keywords:
Thermo-mechanical modelling
Pebble beds
Pebble bed–wall interface
Heat transfer coefficient

ABSTRACT

In HCPB blankets, interfaces between pebble beds and structural material provide for an additional heat resistance, which depends on local mechanical stresses and temperature. The heat transfer coefficient of pebble bed–wall interfaces was investigated by modelling particle–wall contact, radiation effect, and interstitial gas. The predictions of the model were compared to the experimental data. Interfacial modelling as presented by this paper, which takes the coupled thermo-mechanical behaviour of the interface into account, opens up the possibility to implement these effects in a finite element simulation of a structure containing pebble beds.

1. Introduction

In HCPB blankets, pebble beds are used as tritium breeder and neutron multiplier materials. The interaction of pebble beds with structural material is one of the critical issues in the design and analysis of HCPB blankets [1]. Using the phenomenological model of pebble beds discussed in previous investigations [2], structures containing pebble beds, such as HCPB blankets, can be analyzed using coupled thermo-mechanical finite element codes. Before the material model is employed in engineering, however, the interfacial behaviour of interactions between the pebble bed and container wall has to be investigated. The interfacial behaviour is important in coupled thermo-mechanical analyses, since it provides for boundary conditions in the bulk region of the pebble bed in terms of both temperature and displacement.

The pebble–wall interactions may be divided into two categories: (1) mechanical interactions; and (2) the interfacial heat transfer. For mechanical interactions, the interfacial contact and friction forces can be taken into account by a frictional contact law, such as the Coulomb friction law, in the finite element code without spending too much effort for considering the microstructure of pebble beds. As far as the heat transfer coefficient (HTC) between the contacting parts is concerned, however, the microstructure of the pebble beds has to be considered. The HTC depends on the properties of the bulk materials, overall properties of the pebble bed as well as on the temperature and mechanical fields near the interface.

Following a review of experiments and models available, the interfacial heat transfer will be investigated theoretically in Sections 2 and 3, taking into account mechanical contributions. Then, the model prediction will be compared to the experimental data in Section 4. In Section 5, some critical issues will be discussed in detail.

1.1. Experiments

Experimental investigations of heat transfer coefficients for pebble bed–wall interfaces were carried out for ceramic breeder [3–5] and beryllium pebble beds [6,7]. Dalle Donne and Sordon [3] performed experiments to study the interface between a Li_4SiO_4 pebble bed and a stainless steel container. The ceramic pebbles had an average diameter of 0.5 mm and a packing factor of 61.9%. Tehranian et al. [4] and Tehranian and Abdou [5] studied different types of pebble beds in contact with stainless steel, including aluminium pebbles with a diameter of 0.8 mm and packing factor of 63%, and Li_2ZrO_3(lithium zirconate) pebbles with an average diameter of 1.2 mm and packing factor of 65–69%. The purge gas consisted of either air or helium at different pressures. Mechanical load was taken into account, but the average bed temperature was comparably low. For beryllium pebble beds, interfaces were investigated experimentally by Dalle Donne et al. [6] and Abou-Sena et al. [7]. The first type of experiments focusing on the interfaces between a beryllium pebble bed and container wall was carried out in a stainless steel container. Beryllium pebbles had a diameter of 2 mm and two levels of packing factors, namely, 60% and 63% [6]. Due to the experimental set-up, it was not easy to separate the influences of temperature and mechanical loads. Recently, Abou-Sena et al. [7] studied the interfacial heat transfer of a beryllium pebble bed

* Tel.: +49 7247 82 3459.
E-mail address: yixiang.gan@imf.fzk.de (Y. Gan).

0920-3796/$ – see front matter © 2009 Yixiang Gan.. Published by Elsevier B.V. All rights reserved.
doi:10.1016/j.fusengdes.2009.05.003

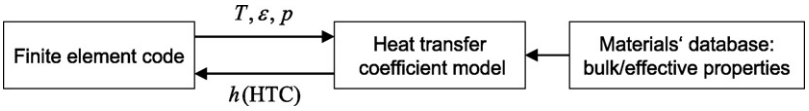

Fig. 1. Interface between the HTC model and a finite element code.

($d = 2$ mm, PF = 60.6%) in contact with a layer of silicon carbide (SiC), including the dependence on both the bed temperature and compressive stresses.

In the above experiments, the basic strategy consisted in extrapolating the temperature measurements by thermo-couples, located inside the pebble bed, to the pebble–wall interface as T_b, and meanwhile measuring the wall temperature T_w. Knowing the surface heat flux q via the interface, the HTC could be expressed as

$$h = \frac{q}{T_b - T_w}. \tag{1}$$

However, inaccuracy of the measurements was introduced by different factors, such as errors of the thermo-couples and the measurement of heat flux q. Another important fact was that the temperature drop through the pebble–wall interface was comparably small due to the limitation of heat supply in the experiments. Therefore, the measurements of the HTC varied over a wide range of magnitudes [3]. A theoretical model of interfacial heat transfer is essential to understand the pebble–wall interactions.

1.2. Available models

Models of interfacial heat transfer were proposed mainly for a packed bed in contact with a flat surface rather than for the specific case of interfaces between pebble beds and wall under fusion-relevant conditions. The latter case includes some specific features, such as the use of high-temperature helium as interstitial gas and a low solid-to-gas conductivity ratio. Still, the basic concepts of these models can be utilized in this investigation.

Of the existing interfacial models, a unit cell is commonly used to study thermal contact conductance of a single spherical particle–wall interaction. Interfacial heat transfer can be separated into different mechanisms, such as heat transfer in the solid–gas region and heat transfer in the solid–solid region. Different assumptions were made with respect to the temperature distribution inside the unit cell, e.g., temperatures at the surfaces of the bulk materials were assumed to be either uniform [8] or non-uniform [9]. Heat transfer through the interstitial gas gap was mostly concerned [8]. Recent models did not only consider the contact between particle and wall, but also the influence of wall materials [10]. In most cases, a parallel heat transfer was assumed in the solid–gas region. As regards the solid–solid contact region, Peterson and Fletcher [11] studied the interface in a vacuum and compared the model with experiments. Gorbis et al. [12] proposed a model based on the near-wall conductivity and studied both solid–gas and solid–solid regions. Except for the work of Kikuchi [10], wall effects were not considered in literature. However, investigation of wall effects is important, if the wall material has a lower thermal conductivity than the bulk material of the pebbles, such as in the case of the interface between beryllium pebble beds and the stainless steel container. For applications in fusion blankets, Reimann et al. [13] investigated the pebble–wall interactions of ceramic and beryllium pebble beds based on Schlünder's model, and this model was proposed to be the reference model for pebble beds. Nevertheless, the solid–solid contact region and wall effects were not taken into account by this model.

Finally, an averaging method was applied to transfer the results from the microscopic study to a phenomenological model. In this way, the HTC model can be combined with a finite element code as shown in Fig. 1. The HTC model needs the definitions of the contacting materials from the material database, i.e., material properties in terms of temperature and state variables from finite element analysis, such as temperature, strains, and stresses. On the other hand, the finite element code needs the HTC value as an input for predicting the current temperature distribution. These procedures are coupled, but an explicit scheme can be adopted in each increment with an adequate time step, e.g., calculating the HTC value with the state variables at the beginning of the time step, and then providing thermal boundary conditions for the finite element code.

2. Modelling of interfacial heat transfer

For heat transfer between two surfaces, the thermal contact conductance (TCC) of the interface is defined as

$$h = \frac{q}{\Delta T}, \tag{2}$$

where q is the surface heat flux through the interface and ΔT is the additional temperature drop due to the presence of the imperfect joint. This concept can be applied directly to study the pebble–wall interaction.

Here, it is focused on pebble–wall interfaces, i.e., interfaces between the pebble bed and container wall. Perpendicular to the interface between the near-wall pebbles and the container wall, an area A containing N contact zones is located (see Fig. 2). These contacting pebbles have a radius of R that is projected onto the interface as dashed circles and the average radius of the contact zones is a. These contact areas are assumed to have the same temperature as the contacting pebbles and they act as "hot spots" on the wall, while heat is transferred from the pebbles to the wall region.

In order to obtain the HTC value of the interface, density of the contact zones has to be taken into account. Here, the parameter

$$L = \left(\frac{A}{\pi N}\right)^{0.5} \tag{3}$$

is used, depending on the near-wall packing structure, which can be either a regular or a random packing of pebbles. To estimate the value of L, the pebbles are assumed to be packed regularly. For the (0 0 1) direction of an FCC packing, the typical value of L/R is $4/\pi$; for the (0 0 1) direction of a BCC packing, it is $16/3\pi$.

Considering the condition of axisymmetry, a basic unit cell can be sketched, as shown in Fig. 3(a). This is a microscopic side view of

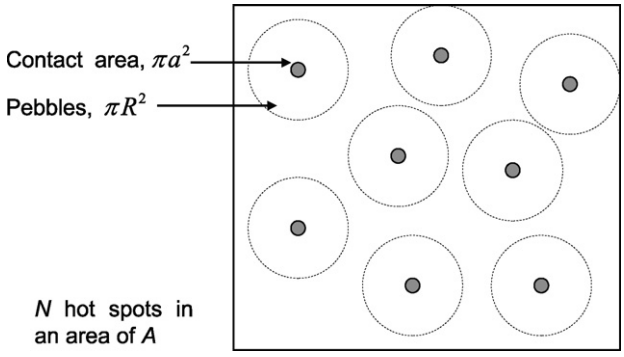

Fig. 2. Multiple "hot spots" model for thermal contact conductance.

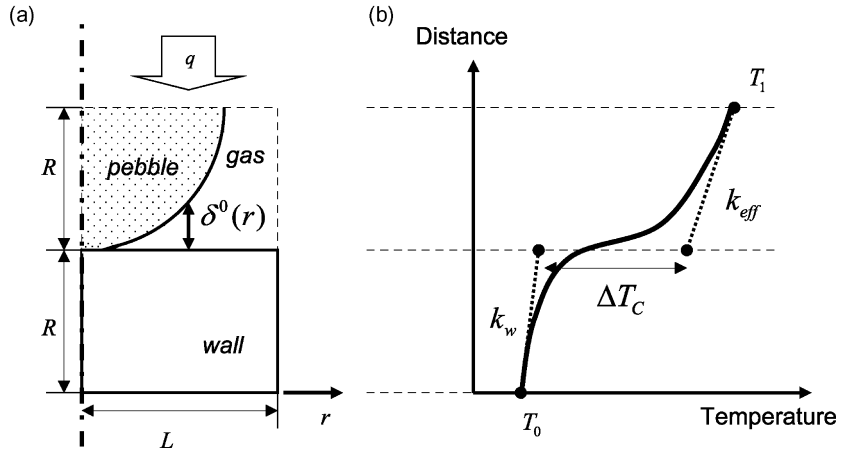

Fig. 3. (a) The unit cell of the HTC model and (b) temperature distribution.

each contact zone and includes the regions of the wall, pebble, and interstitial gas. The pebble has a radius of R and the unit cell has a thickness of $2R$. The radius of the unit cell is L and depends on the topology of the packed pebbles near the wall, as defined by Eq. (3). $L = 4R/\pi$ is used in this unit cell.

Temperature distribution along the direction perpendicular to the interface, representing the temperature averaged in r-direction at each cross-section, is schematically drawn in Fig. 3(b). The two temperature values at the upper and lower boundaries of the unit cell, denoted as T_1 and T_0, respectively, are connected by a solid curve that reflects the actual temperature distribution. Two dashed lines indicate the temperature distributions extrapolated by the thermal conductivity of wall material, k_w, and the effective thermal conductivity of the pebble bed, k_{eff}, respectively. The temperature difference ΔT_C at the interface is calculated by the difference of these two extrapolated temperatures and corresponds to the additional temperature drop due to the presence of the interface. If Q is the total heat flow through the unit cell, then the heat transfer coefficient can be expressed as

$$h = \frac{Q}{\pi L^2 \, \Delta T_C} = \frac{q}{\Delta T_C}. \tag{4}$$

In principle, heat transfer via an interface occurs by a combination of four different modes: conduction through the pebble–wall contacts, conduction through the interstitial gas, convection in the interstitial gas region, and thermal radiation. Researchers [14] pointed out that the convection mode usually is negligible for gap widths of up to 6 mm (corresponding to a Grashof number of 2000 for air at atmospheric pressure of 101 kPa and a temperature of 300 K). A similar conclusion was drawn by Yagi and Kunii [15]. In the case of helium being the interstitial purge gas, as in fusion blankets, the convection mode hence is negligible.

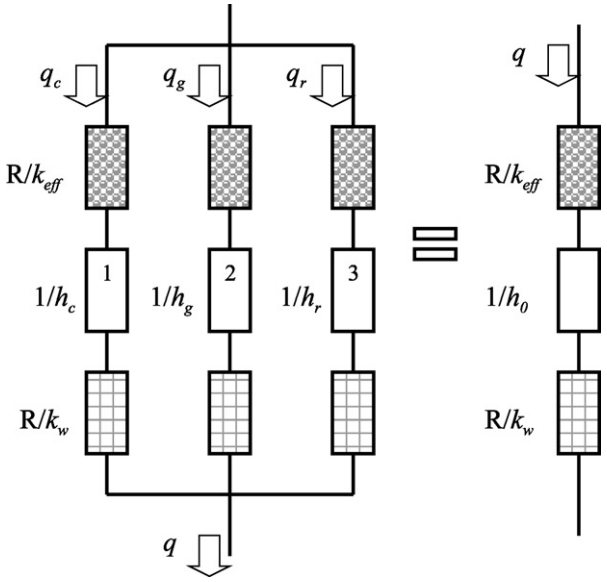

Fig. 5. Electrical analog of thermal conductances in Fig. 4.

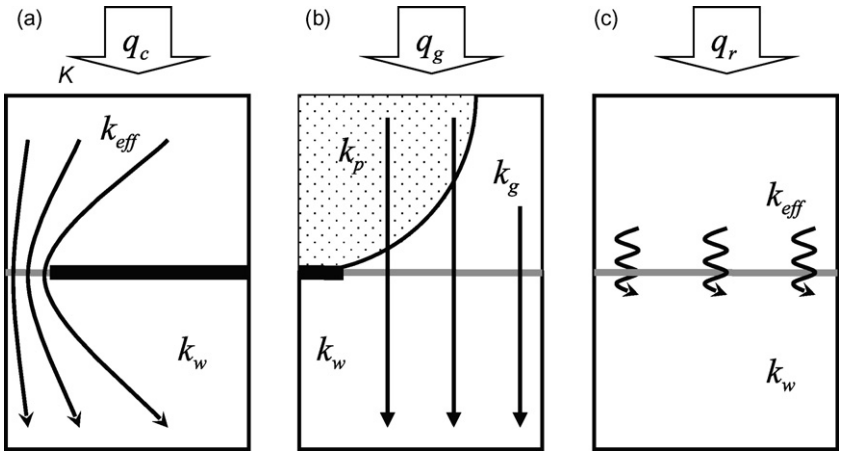

Fig. 4. Three mechanisms of heat transfer in the unit cell.

Heat flux q through the unit cell is split up into three main mechanisms in Fig. 4: (a) q_c, heat transfer through the solid–solid contact; (b) q_g, through the gas gap; and (c) q_r, by thermal radiation. These types of heat flux fulfill the condition

$$q = q_c + q_g + g_r. \tag{5}$$

In Fig. 4, k_{eff}, k_p, k_w, and k_g indicate the effective thermal conductivity of pebble beds, as well as the thermal conductivities of the bulk material of pebbles, wall material, and interstitial gas, respectively.

Since the equations of thermal conduction have a form similar to that of Ohm's law, these types of thermal conduction can be summed in the same manner as serial and parallel electrical conductors. The electrical analogous problem here is sketched in Fig. 5. Inside each mechanism, the thermal resistors are connected in series, while for the three different mechanisms, the overall resistors are connected in parallel. It is aimed at finding the solution of the interfacial heat transfer coefficient h_0 in the relation

$$\sum_{i=c,g,r} \left(\frac{R}{k_{\text{eff}}} + \frac{1}{h_i} + \frac{R}{k_w} \right)^{-1} = \left(\frac{R}{k_{\text{eff}}} + \frac{1}{h_0} + \frac{R}{k_w} \right)^{-1}. \tag{6}$$

The different mechanisms will be analyzed in the following section. From Eq. (6), the heat transfer coefficient of the interface, h_0, can be obtained.

3. Analysis of the unit cell

In this section, three different mechanisms will be analyzed separately to obtain the overall behaviour of the unit cell. Heat transfer through each pebble–wall unit cell at the interface is assumed to be identical. Consequently, the phenomenological heat transfer coefficient is obtained directly from the unit cell.

3.1. Solid–solid region

The first mechanism of interfacial heat transfer is conduction via pebble–wall contact in the unit cell. To solve the problem analytically, the change of the mechanical field resulting from the compressive stress present at the interface, p_n, has to be taken into account. If the interface has a surface normal $\mathbf{n}$, $p_n = \boldsymbol{\sigma} \cdot \mathbf{n}$. According to the Hertzian solution [16], the radius of the contact zone and the contact force $P = p_n(\pi L^2)$ are related as follows

$$a = \left[\frac{3}{4} \pi P (K_p + K_w) R \right]^{1/3}, \tag{7}$$

where K_p and K_w depend on the elastic moduli of the bulk materials, as $K_i = (1 - \nu_i^2)/\pi E_i$ with $i = p, w$.

In the solid–solid region, Madhusudana [17] provided a solution for thermal conductance of the solid spot contact as a function of the contact area

$$h_c = \frac{2ak}{\pi L^2}. \tag{8}$$

Here, $k = 2k_w k_p/(k_w + k_p)$ is the harmonic mean of the bulk thermal conductivities of wall and pebble and a is the radius of the contact spot in Eq. (7).

Peterson and Fletcher [11] investigated interfacial heat transfer in a vacuum experimentally, which resulted in the summation of the contributions of solid–solid contacts and thermal radiation. The analytical result of solid contact conductance fits well to the experiments, since the contribution of thermal radiation is relatively small.

3.2. Solid–gas region

For heat transfer via the gas gap as illustrated in Fig. 4(b), the overall heat conductance $h^{(b)}$is

$$h^{(b)} = \left(\frac{R}{k_{\text{eff}}} + \frac{1}{h_g} + \frac{R}{k_w} \right)^{-1}. \tag{9}$$

In this region, $h^{(b)}$ can be obtained directly from the analysis of the unit cell instead of calculating h_g.

As shown in Fig. 3(a), the distance between the two surfaces at the same radial position r can be expressed as

$$\delta^0(r) = \begin{cases} R - \sqrt{R^2 - r^2}, & r < R, \\ R, & L \geq r \geq R. \end{cases} \tag{10}$$

This expression is valid, if the bulk materials of pebble and wall are hard materials, and, hence, the gap reduction due to compressive stresses is negligible over a certain range of mechanical load. Otherwise, gap reduction can be taken into account by the relative displacement between the contacted surfaces.

To study heat transfer via a interstitial gas gap, general properties of the gas gap have to be considered first. For the gas gap, thermal conductivity in the microscopic region near the solid surface decreases due to the Smoluchowski effect. This effect accounts for the inefficiency of energy exchange between gas molecules and solid surfaces during single collisions [17]. Thus, thermal conductivity of a gas gap with a width of $\delta^0(r)$ reads as

$$k_g(r) = \frac{k_{g,\infty}}{1 + (\Delta + j)/\delta^0(r)}, \tag{11}$$

where $k_{g,\infty}$ is the thermal conductivity of gas without the effect of solid–gas interfaces and Δ is the summation of surface roughness. The coefficient j is the temperature jump distance, taking into account the Smoluchowski effect. In a sufficiently large gas gap, the Smoluchowski effect vanishes. The temperature jump distance can be expressed as

$$j = \left(\sum_i \frac{2 - \alpha_i}{\alpha_i} \right) \frac{2\gamma}{\gamma + 1} \frac{\lambda}{Pr}, \tag{12}$$

where α_i denotes the accommodation coefficient of the interstitial gas on the corresponding surface, γ is the ratio of specific heats, λ is the mean free path of gas molecules, and Pr is the Prandlt number. The mean free path λ_g of gas molecules at temperature T_g and pressure p_g is related to λ_0 as

$$\lambda_g = \lambda_0 \left(\frac{T_g}{T_0} \right) \left(\frac{p_0}{p_g} \right), \tag{13}$$

at temperature T_0 and pressure p_0. It was suggested by Song and Yovanovich [18] that the accommodation coefficient $\alpha = 0.4$ can be used for most engineering surfaces to give a reasonable approximation.

In the solid–gas region, different assumptions can be made with respect to the heat transfer. The interstitial gas gap was studied under the following assumptions by Schlünder [8]: (1) temperature on each surface is uniform; (2) temperature difference between two different surfaces corresponds to the additional temperature drop ΔT_C of the unit cell; and (3) heat flow is one-dimensional. This gives the heat transfer coefficient as

$$h^{(b)} = \frac{1}{\pi L^2} \int_a^L \frac{k_g(r)}{\delta^0(r)} 2\pi r \, \mathrm{d}r. \tag{14}$$

It is valid in case of $k_g \ll k_p$ and $k_g \ll k_w$. This expression can be used for packed beds and yields reasonable results, although it was assumed that all contacts are point-wise and the surfaces

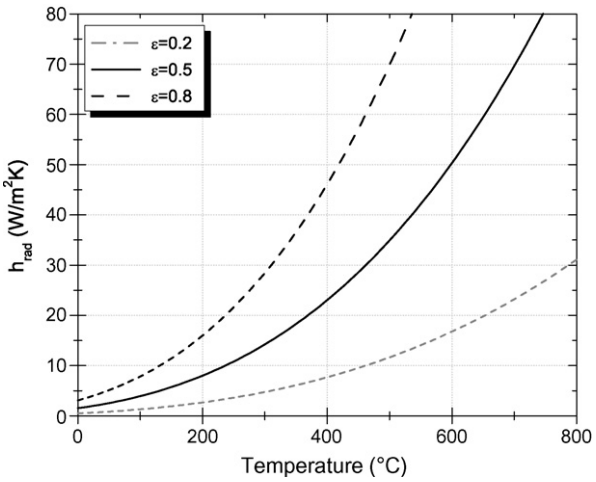

Fig. 6. Radiation effect as a function of temperature.

have zero roughness [8]. In other words, this model does not separate the effects of the solid–solid and solid–gas regions. As a result, the model may yield an overestimation, if the solid–gas region is considered only.

Alternatively, heat transfer may be assumed to follow parallel heat pipes from the top to the bottom of the unit cell [9]. Compared with the assumptions made by Schlünder [8], assumption (1) has been released, so the temperature distributions on the surfaces can be position-dependent; assumption (2) is irrelevant in this case; assumption (3) remains and parallel heat transfer is also assumed in this case. This model considers the effects of both the wall and the bulk region of pebbles. The corresponding heat transfer coefficient in the solid–gas region is

$$h^{(b)} = \frac{1}{\pi L^2}\int_a^L \frac{1}{(R-\delta^0(r))/k_p + \delta^0(r)/k_g(r) + R/k_w} 2\pi r\,\mathrm{d}r. \qquad (15)$$

Both types of assumptions give comparable predictions of the heat transfer coefficient, while the value obtained by the second one is smaller, especially for materials with a low solid-to-gas conductivity ratio. Therefore, for ceramic breeder pebble beds, the Schlünder model usually gives an overestimation. In this investigation, the second type of modelling is used for the solid–gas region.

3.3. Radiation effect

For thermal radiation, the heat transfer coefficient depends on the mean temperature of the interface, T_i, as

$$h_r = 4\frac{C_s}{1/\epsilon_w + 1/\epsilon_p - 1}T_i^3 \qquad (16)$$

where C_s is the Stefan–Boltzman constant ($5.67\times10^{-8}\,\mathrm{W/m^2\,K^4}$), ϵ_w is the emissivity of the wall, and ϵ_p is the emissivity of pebble bed. Fig. 6 shows the radiation effects as a function of temperature, with different values of emissivity. In this investigation, $\epsilon_w = \epsilon_p = 0.5$. The radiation effect is negligible in the low-temperature region, which was also found in the experiments [11].

3.4. Overall behaviour

By inserting the solutions of h_c, h_g (or $h^{(b)}$), and h_r into Eq. (6), the value of h_0 is obtained. This solution represents the dependence on temperature, gas pressure, and mechanical stress. By implementing this relation in the finite element code, the heat transfer coefficient can be realized in a fully coupled thermo-mechanical analysis.

Table 1
Properties of bulk materials for heat transfer coefficients.

Bulk material	Thermal conductivity (W/mK)	Young's modulus (GPa)	Poisson's ratio
Beryllium	176.95	287	0.032
Li_4SiO_4	1.42	90	0.24
Stainless steel	14.15	196	0.30
SiC	45	450	0.21

Table 2
Parameters for the thermal conductivity of the gas gap.

Thermal conductivity $k_{g,\infty}$ (W/mK)	$3.623\times10^{-3}\times T(K)^{0.66}$
Ratio of specific heats, γ	1.66
Prandtl number, Pr	0.67
Accommodation coefficient, α	0.4
Mean free path of gas molecules, λ (nm)	0.186 ($T_0 = 300$ K, $p_0 = 101$ kPa)

Table 3
Correlations of the effective thermal conductivities of pebble beds.

	Types	Thermal conductivity	Ref.
Be	$d = 2$ mm; $PF = 63\%$.	$2.499 + 2.07\times10^{-3}T_m$	[6]
	$d = 2$ mm; $PF = 60\%$.	$1.823 + 2.053\times10^{-3}T_m$	[6]
	$d = 2$ mm; $PF = 60.6\%$.	$1.9712 + 2.2\times10^{-3}T_m$	[7]
Li_4SiO_4	$d = 0.5$ mm; $PF = 61.9\%$.	0.736 ($T_m = 51.6$); 0.825 ($T_m = 131.6$)	[3]

4. Comparison with the experiments

The heat transfer coefficient depends on the additional temperature drop ΔT_C at the interface, which typically is small and not easy to measure in experiments. Only a few measurements are available for Li_4SiO_4 and beryllium pebble beds in literature [3,6,7]. In this section, the prediction of the theoretical model shall be compared to the experimental data available.

4.1. Material parameters

In the present HTC model, material properties are required for the purpose of validation. To facilitate prediction, temperature dependence of the bulk material properties is not taken into account, since its effect is moderate.[1] Hence, temperature dependence of the heat transfer coefficient is dominated by the interstitial gas phase. Table 1 shows the properties of the bulk materials used in this investigation.[2] Table 2 shows the parameters for the thermal conductivity of the gas gap, with helium being chosen as the interstitial purge gas. Surface roughness (Δ) of these materials is set to 5 μm. The effective thermal conductivities (k_{eff}) of pebble beds are listed in Table 3. Here, the unit of k_{eff} is (W/mK); T_m (°C) is the mean temperature of the pebble bed; d is the mean diameter of pebbles; PF denotes the packing factor; and $\varepsilon(\%)$ is the compressive strain. These measurements of k_{eff} in Table 3 were made in the same experiments to obtain the heat transfer coefficients. The reference effective thermal conductivities can be found in Refs. [19,20,13] for both Li_4SiO_4 and beryllium pebble beds.

4.2. Comparison with available experiments

Table 4 summaries the experimental HTC results, where T_w (°C) is the near-wall temperature of the pebble bed. Depending on the

[1] For parameter study, a case with Li_4SiO_4/stainless steel interface has been investigated: increasing the bulk thermal conductivity of the wall material by 10% will bring an increase of HTC of 0.1%; while increasing the thermal conductivity of bulk Li_4SiO_4 by 10% will bring an increase of HTC of 5%. Therefore, we state that temperature dependence of the bulk material properties is moderate.

[2] Data from *Fusion Network*: http://fusionnet.seas.ucla.edu/fusionnetwork/index.php, and the bulk material properties are calculated at room temperature.

Table 4
Heat transfer coefficients of pebble–wall interactions.

	Types	HTC (W/m^2 K)	Ref.
Be	$d = 2$ mm; $PF = 63\%$.	$369 + 0.8666T_w + 3.472 \times 10^{-3}T_w^2$ (Be/stainless steel)	[6]
	$d = 2$ mm; $PF = 60\%$.	$614.6 - 0.8867T_w + 7.899 \times 10^{-3}T_w^2$ (Be/stainless steel)	[6]
	$d = 2$ mm; $PF = 60.6\%$.	data points (Be/SiC)	[7]
Li_4SiO_4	$d = 0.5$ mm; $PF = 61.9\%$.	data points (Li_4SiO_4/stainless steel)	[3]

bulk materials, three types of experiments can be distinguished: experiments focussing on the Be/stainless steel interface [6], the Be/SiC interface [7], and the Li_4SiO_4/stainless steel interface [3]. The above material properties as well as the effective thermal conductivity of pebble beds are used as inputs of the present interfacial model.

4.2.1. Be/stainless steel

Fig. 7 compares the present HTC model and experimental results for the Be/stainless steel interface. This type of experiments was performed in PEHTRA [6], with a cylindrical container and a rod heater located in the center. It is difficult to control the thermal stresses induced by the temperature change. Heat conductance at high temperatures increases not only because of the changing thermal conductivity of the interstitial gas with temperature, but also due to the induced compressive stresses at the interface. A small increase of the compressive stresses may cause noticeable changes of the HTC value, since beryllium has a relatively high-thermal conductivity. Although the model overestimates the value at low temperatures, it still gives reasonable predictions, including temperature dependence and the difference between the two cases with different packing factors. At the same temperature level, the case with a packing factor of 60% has a higher HTC value than the one with a packing factor of 63% for both experiments and predictions. The unit cell at the near-wall region for both cases with different packing factors are identical, which indicates that the right hand side of Eq. (6) is the same. However, the denser packed bed has higher effective thermal conductivity, k_{eff}, as shown in Table 3. As a result, a lower value of HTC is expected in the case with PF =63%.

4.2.2. Be/SiC

Predictions and experiments regarding the Be/SiC interface are compared in Fig. 8. Abou-Sena et al. [7] performed a series of measurements to investigate: (i) the dependence on the mean bed temperature and (ii) the dependence on the pressure at a fixed bed temperature. Fig. 8(a) shows that the HTC changes over the mean bed temperature, from room temperature to 450 °C. In Fig. 8(b), the pressure varies from 0 to 2 MPa at a mean bed temperature of 270 °C. The prediction shows a clear increase of HTC with respect to the mechanical pressure. An overestimation of the theoretical model is also found in this case.

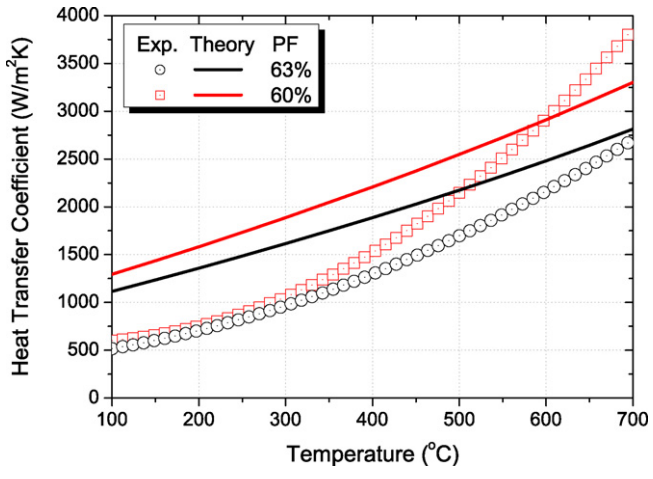

Fig. 7. Comparison of the HTC model with data from Ref. [6]: the Be/stainless steel interface.

4.2.3. Li_4SiO_4/stainless steel

The experimental data are limited for the Li_4SiO_4/stainless steel interface [3]. Again, a cylindrical container with a heater rod in its center is used. Two data points are measured near the heater side (the inner wall), and the remaining measurements are performed near the coolant side (the outer wall). The model and measurements are compared in Fig. 9(a). It has been suggested that these data from the inner wall are more reliable, due to the presence of larger temperature drops [3]. The outer wall exhibits smaller temperature drops, as a consequence of which the HTC is difficult to be determined. The level of the compressive stresses inside the container is not clear. Hence, the prediction of uncompressed pebble beds is used, similar to the case of the Be/stainless steel interface. Predictions of the HTC model here are below the experimental data on the heater side and above the experimental data on the coolant side. The predictions of Li_4SiO_4/stainless steel interface are shown in Fig. 9(b), with effective thermal conductivity of the bed from Refs. [3,13], respectively. However, the existing experimental data points are scattered as shown in Fig. 9(a), further experimental investigation on Li_4SiO_4/stainless steel interface will be necessary.

5. Discussion

The differences between the predictions by the HTC model and experimental data were outlined in the previous section. Now, the accuracy of both the theoretical model and the experimental measurements shall be discussed.

5.1. Predictions and experimental measurements

(1) One explanation for the error introduced by experiments is, as sketched in Fig. 10(a), the difference between the real temperature distribution (dashed curve) and the extrapolated one (solid line) inside the pebble bed. The additional temperature drop ΔT_C is calculated by the difference between the near-wall temperature T_n and wall temperature $T_{w,n}$, where $n = 1, 2$ indicates the position of the interface. The mean temperature of the bed is denoted by T_m obtained by integration over the true temperature distribution. The effective thermal conductivity of the pebble bed is considered to be a monotonically increasing function of temperature. For the temperature distribution extrapolated by using $k_{\text{eff}}(T_m)$ and represented by the solid line, this introduces larger ΔT_C on the low-temperature side and smaller ΔT_C on the high-temperature side. This phenomenon can also be observed in the experimental results provided by Ref. [3]: the outer wall measurements of the HTC are much smaller than those near the inner wall, as shown in Fig. 9(a). However, the magnitudes of these two types of measurements are supposed to be comparable.

A similar simplification is made in the theoretical model during validation. To extrapolate the temperature inside the unit cell, the effective thermal conductivity can be used as a function of either the mean temperature of the bed or the local temperature, as in Fig. 10(b). In experiments, the mean temperature has been used. Therefore, the effective thermal conductivity k_{eff} is estimated and used for comparison as a function of the mean bed temperature T_m to compare with experiments. In practice, however, the near-wall temperature T_n should be used. The difference is pronounced for pebble beds having low effective

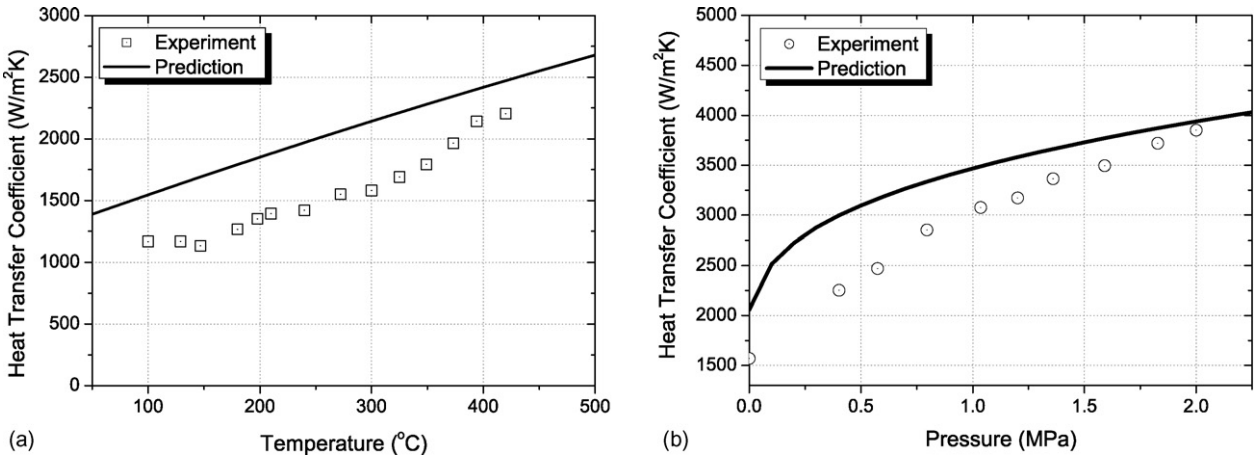

Fig. 8. Comparison of the HTC model with data from Ref. [7]: the Be/SiC interface. HTC versus: (a) the mean bed temperature and (b) compressive stresses ($T_m = 270\,^{\circ}C$).

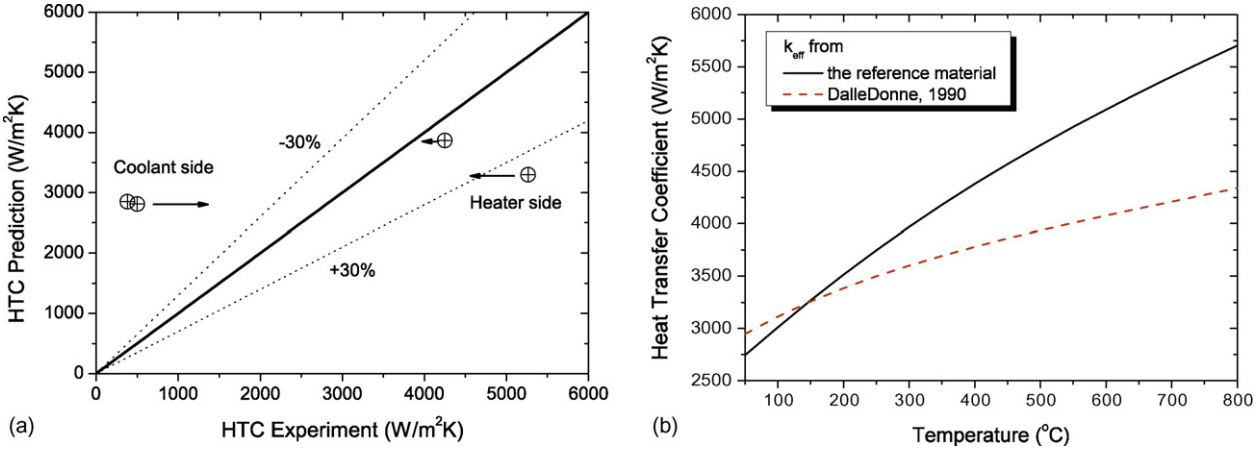

Fig. 9. Li_4SiO_4/stainless steel interface: (a) comparison of the HTC model with data from Ref. [3]. (b) HTC model versus the near-wall temperature, with the effective thermal conductivity of the bed from Ref. [3](dashed line) and Ref. [13](solid line).

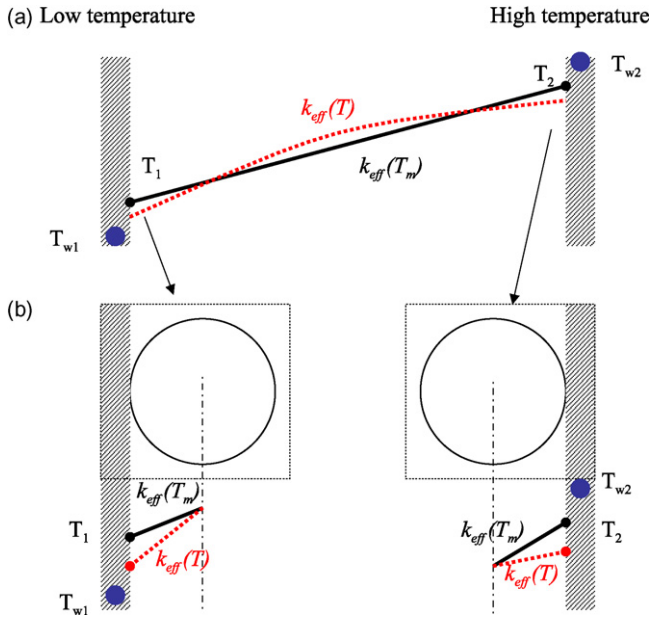

Fig. 10. (a) Schematic representation of temperature distributions and (b) the near-wall regions.

thermal conductivities and, thus, larger values of $|T_m - T_n|$. This effect in the near-wall regions results in an overestimation near the high-temperature region, and an underestimation near the low-temperature region.

(2) Furthermore, the gas properties depend on the local temperature, as shown in Table 2. Use of the near-wall temperature T_n instead of the local interstitial gas temperature T_g leads to additional errors. Since the gas has lower thermal conductivity than the bulk material of pebble, in a pebble bed, $T_g < T_n$ on the heater side and $T_g > T_n$ on the coolant side. For instance, if thermal conductivity of the interstitial gas is a monotonically increasing function of temperature, the present model overestimates the HTC value at the high-temperature region and vice versa.

(3) Except for the experiments conducted by Ref. [7], the mechanical field was not separated from the temperature field. However, the size of the contact zone is important to the beryllium pebble–wall interactions, as shown in Fig. 8(b). With more information from experiments, the predictions of the present model can be validated better. Moreover, changes of the average coordination number in the bulk region are observed by discrete element simulations [21]. In addition, the stress state may cause a variation of the contact number between pebbles and the wall during heating. In the theoretical model, however, the contact number was fixed as an intermediate value ($L/R = 4/\pi$), which results in an overestimation in the region with low compressive stresses

Table 5
Factors influencing the predictions of the present HTC model.

Influencing factors	Low temperature	High temperature
(1) Eff. thermal cond. using T_m [a]	Underestimation	overestimation
(2) Gas properties using T_w	Underestimation	Overestimation
(3) Without compressive stress	Underestimation	Underestimation
(4) Near-wall topology	Overestimation	Overestimation

[a] For both the theoretical model and experiments.

and an underestimation in the region with high-compressive stresses.

(4) According to the HTC model with a unit cell, k_{eff} is independent of the near-wall packing, except for the first (1/2) diameter region near the wall. Nevertheless, the changes of topology are found mainly in the region of 4 diameters away from the wall [22]. Recently, it was possible to investigate how the packing factor changes near the wall by means of microtomography [23,24]. The effective thermal conductivity could be varied and most likely decreased, but the influence is not yet clear. Accordingly, the HTC model may yield an overestimation compared to the real situation.

The above facts influencing the accuracy of the predictions are listed in Table 5. Despite the fact that the current model already is in reasonable agreement with the experimental observations, the influences of factors (1)–(3) can be eliminated if more information will be obtained in further experiments. For instance, T_n and T_g can be derived from the experimental data as a function of T_m and moreover, the compressive stresses can be observed explicitly [7]. Here, The reasons of inaccuracies during validation were discussed.

However, for a fully coupled thermo-mechanical analysis of the structure containing pebble beds, local temperature and stress state can be obtained and considered in the interfacial model. In this way, the influences of (1) and (3) are eliminated. In engineering applications, the prediction of the present theoretical model, h_0, usually represents an overestimation, such as in the benchmark exercises of HELICA and HEXCALIBER. It is suggested to use $\bar{h} = \alpha h_0 (\alpha < 1)$ to calibrate the heat transfer coefficient. For example, a value of α =0.6–0.8 has been used in the analyses of the HELICA and HEXCALIBER benchmark exercises [25,26].

5.2. Gap formation

In the case of gap formation, a layer of interstitial gas can be added to the unit cell. The solid–solid region is removed, and gap formation is taken into account by varying the thickness of the gas gap. A simplified model can be written as

$$\bar{h}_0 = \left(\frac{1}{h_0} + \frac{\delta}{k_{g,\infty}} \right)^{-1}, \tag{17}$$

where δ is the thickness of the additional gas gap, and h_0 is the solution of the unit cell without the solid–solid region.

In spite of the simplification made in the theoretical model, it gives reasonable predictions. The model has been implemented in ABAQUS, coupled with the phenomenological model for the bulk region of pebble beds, to perform thermo-mechanical analyses of HCPB blankets under fusion-relevant conditions.

6. Conclusion

In this paper, heat transfer via the pebble–wall interface was investigated theoretically. A model to estimate the interfacial heat transfer coefficient based on the temperature and mechanical fields was proposed. In this model, a unit cell, consisting of a solid–solid region, a solid–gas region, and thermal radiation, was analyzed. Comparisons were made to validate the present HTC model to the available experiments. The differences between predictions and experimental data were explained by discussing the current HTC model. This model can be implemented straightforwardly in a finite element code to perform fully coupled thermo-mechanical analyses of structures taking into account pebble beds.

Acknowledgments

This work, supported by the European Communities under the contract of Association between EURATOM and Forschungszentrum Karlsruhe, was carried out within the framework of the European Fusion Development Agreement. The views and opinions expressed herein do not necessarily reflect those of the European Commission.

References

[1] J. Reimann, L. Boccaccini, M. Enoeda, A.Y. Ying, Thermomechanics of solid breeder and Be pebble bed materials, Fusion Engineering and Design 61 (2) (2002) 319–331.
[2] Y. Gan, M. Kamlah, Identification of material parameters of a thermo-mechanical model for pebble beds in fusion blankets, Fusion Engineering and Design 82 (2) (2007) 189–206.
[3] M. Dalle Donne, G. Sordon, Heat-transfer in pebble beds for fusion blankets, Fusion Technology 17 (4) (1990) 597–635.
[4] F. Tehranian, M.A. Abdou, M.S. Tillack, Effect of external pressure on particle bed effective thermal conductivity, Journal of Nuclear Materials 215 (1994) 885–890.
[5] F. Tehranian, M.A. Abdou, Experimental study of the effect of external-pressure on particle bed effective thermal properties, Fusion Technology 27 (3) (1995) 298–313.
[6] M. Dalle Donne, A. Goraieb, G. Piazza, F. Scaffidi-Argentina, Experimental investigations on the thermal and mechanical behaviour of single size beryllium pebble beds, Fusion Technology 38 (3) (2000) 290–298.
[7] A. Abou-Sena, A. Ying, M. Abdou, Experimental investigation and analysis of the effective thermal properties of beryllium packed beds, Fusion Science and Technology 44 (1) (2003) 79–84.
[8] E.U. Schlünder, Particle heat transfer, in: Proceeding of the 7th International Heat Transfer Conference, vol. 1, Hemishere, Publ. Co, München, Germany, 1982, pp. 195–212.
[9] G.R. McGee, M.H. Schankula, M.M. Yovanovich, Thermal resistance of cylinder-flat contacts: theoretical analysis and experimental verification of a line-contact model, Nuclear Engineering and Design 86 (3) (1985) 369–381.
[10] S. Kikuchi, Numerical analysis model for thermal conductivities of packed beds with high solid-to-gas conductivity ratio, International Journal of Heat and Mass Transfer 44 (6) (2001) 1213–1221.
[11] G.P. Peterson, L.S. Fletcher, Thermal contact conductance of packed-beds in contact with a flat surface, Journal of Heat Transfer-Transactions of the ASME 110 (1) (1988) 38–41.
[12] Z.R. Gorbis, M.S. Tillack, F. Tehranian, M.A. Abdou, Analysis of wall-packed bed thermal interactions, Fusion Engineering and Design 27 (1995) 216–225.
[13] J. Reimann, R. Knitter, G. Piazza, New compilation of the material data base and the material assessment report, Final report on TW5-TTBB-006-D02, Technical report, 2005.
[14] P.M. Lang, Calculating heat transfer across small gas-filled gaps, Nucleonics 20 (1) (1962) 62–63.
[15] S. Yagi, D. Kunii, Studies on heat transfer near wall surface in packed beds, AIChE Journal 6 (1) (1960) 97–104.
[16] K.L. Johnson, Contact Mechanics, Cambridge University Press, Cambridge, 1985.
[17] C.V. Madhusudana, Thermal Contact Conductance, Springer, 1995.
[18] S. Song, M.M. Yovanovich, Correlation of thermal accommodation coefficient for 'engineering' surfaces, in: Proceedings of the Twenty-fourth National Heat Transfer Conference and Exhibition, Pittsburgh, PA, August 9–12 (A88-18501 05-34), American Society of Mechanical Engineers, New York, 1987, pp. 107–116.
[19] J. Reimann, S. Hermsmeyer, Thermal conductivity of compressed ceramic breeder pebble beds, Fusion Engineering and Design 61 (2) (2002) 345–351.
[20] J. Reimann, G. Piazza, H. Harsch, Thermal conductivity of compressed beryllium pebble beds, Fusion Engineering and Design 81 (1–7) (2006) 449–454.
[21] Y. Gan, Thermo-mechanics of pebble beds in fusion blankets, Ph.D. thesis, Universität Karlsruhe, FZKA-7455, 2008.
[22] W.A. Gray, The Packing of Solid Particles, Chapman and Hall, 1968, p. 7455.

[23] J. Reimann, R.A. Pieritz, R. Rolli, Topology of compressed pebble beds, Fusion Engineering and Design 81 (1–7) (2006) 653–658.
[24] J. Reimann, R.A. Pieritz, C. Ferrero, M. Di Michiel, R. Rolli, X-ray tomography investigations on pebble bed structures, Fusion Engineering and Design 83 (7–9) (2008) 1326–1330.
[25] Y. Gan, M. Kamlah, Thermo-mechanical analysis of pebble beds in HELICA mock-up experiments, Fusion Engineering and Design 83 (7–9) (2008) 1313–1316.
[26] Y. Gan, M. Kamlah, Thermo-mechanical analyses of HELICA and HEXCALIBER mock-ups, Journal of Nuclear Materials 386–388 (2009) 1060–1064.